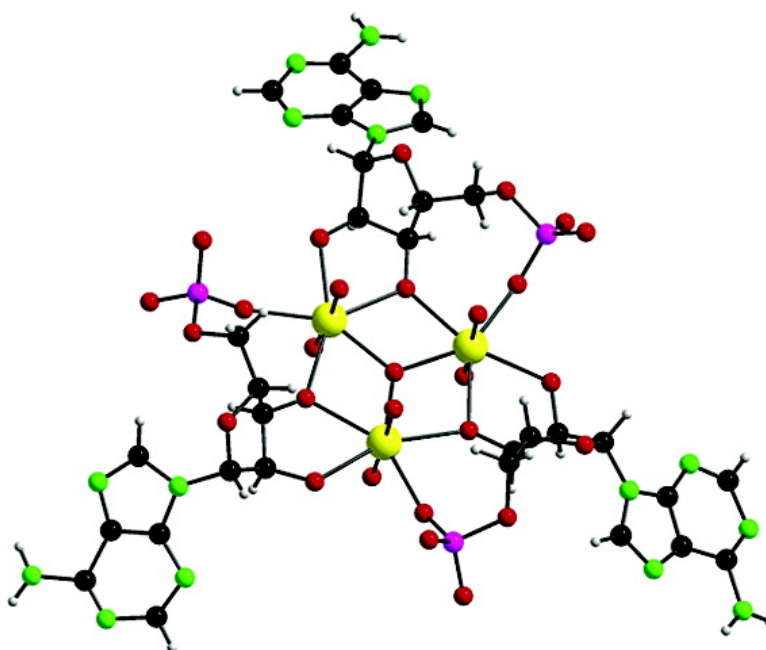


## Combinatorial Multinuclear NMR and X-ray Diffraction Studies of Uranium(VI)-Nucleotide Complexes

Zoltn Szab, Istvn Fur, and Ingeborg Csregh

*J. Am. Chem. Soc.*, **2005**, 127 (43), 15236-15247 • DOI: 10.1021/ja0550273 • Publication Date (Web): 08 October 2005

Downloaded from <http://pubs.acs.org> on March 25, 2009



### More About This Article

Additional resources and features associated with this article are available within the HTML version:

- Supporting Information
- Links to the 1 articles that cite this article, as of the time of this article download
- Access to high resolution figures
- Links to articles and content related to this article
- Copyright permission to reproduce figures and/or text from this article

[View the Full Text HTML](#)



**ACS Publications**  
High quality. High impact.

### Combinatorial Multinuclear NMR and X-ray Diffraction Studies of Uranium(VI)-Nucleotide Complexes

Zoltán Szabó,<sup>\*,†</sup> István Furó,<sup>‡</sup> and Ingeborg Csöreg<sup>§</sup>

Contribution from Inorganic Chemistry and Physical Chemistry, Department of Chemistry, Royal Institute of Technology (KTH), S-10044 Stockholm, Sweden, and Department of Structural Chemistry, Arrhenius Laboratory, Stockholm University, S-106 91 Stockholm, Sweden

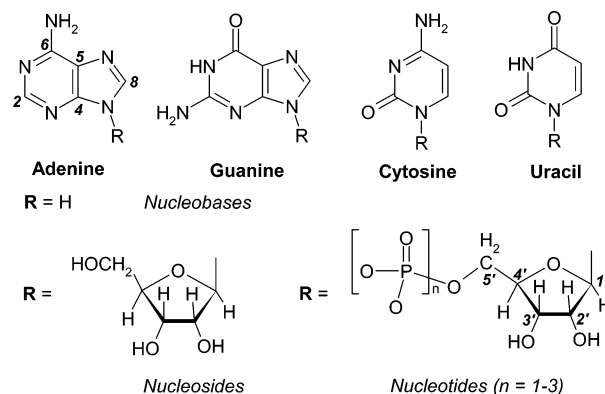
Received July 26, 2005; E-mail: zoltan@kth.se

**Abstract:** The complex formation of uranium(VI) with four nucleotides, adenosine- (AMP), guanosine- (GMP), uridine- (UMP), and cytidine-monophosphate (CMP), has been studied in the alkaline pH range (8.5–12) by <sup>1</sup>H, <sup>31</sup>P, <sup>13</sup>C, and <sup>17</sup>O NMR spectroscopy, providing spectral integral, chemical shift, homo- and heteronuclear coupling, and diffusion coefficient data. We find that two and only two complexes are formed with all ligands in the investigated pH region independently of the total uranium(VI) and ligand concentrations. Although the coordination of the 5'-phosphate group and the 2'- and 3'-hydroxyl groups of the sugar unit to the uranyl ions is similar to that proposed earlier ("Feldman complex"), the number and the structures of the complexes are different. The uranium-to-nucleotide ratio is 6:4 in one of the complexes and 3:3 in the other one, as unambiguously determined by a combinatorial approach using a systematic variation of the ratio of two ligands in ternary uranium(VI)-nucleotide systems. The structure of the 3:3 complex has been determined by single-crystal diffraction as well, and the results confirm the structure proposed by NMR in aqueous solution. The results have important implications on the synthesis of oligonucleotides.

#### Introduction

Metal ions play a key role in several important biological processes,<sup>1–3</sup> and their interaction with nucleotides and other orthophosphoric acid esters in living systems has received considerable attention.<sup>4–11</sup> The information-carrying nucleic acids (DNA, RNA) and nucleotides (e.g., AMP, ATP) are prominent representatives of these esters. Adenosine, guanosine, cytidine, and thymidine phosphates are the four most important nucleotides found in nature. As shown in Scheme 1, they consist of a sugar moiety bound to a heterocycle that is converted to nucleotides upon phosphorylation. The investigation of the structure and stability of these metal complexes in solution has relevance for the understanding of metabolic processes and drug actions.<sup>1–3</sup>

#### Scheme 1



The interaction between uranium(VI) and nucleotides and nucleic acids has been intensively studied; two aspects are of particular importance. A number of studies focused on the application of uranium(VI) as catalyst in the synthesis of 2'-5'-linked oligonucleotides with high regio- and stereo-selectivity.<sup>12–17</sup> Another intensively studied field is the applica-

<sup>†</sup> Inorganic Chemistry, Royal Institute of Technology.

<sup>‡</sup> Physical Chemistry, Royal Institute of Technology.

<sup>§</sup> Stockholm University.

- (1) Kendrick, M. J.; May, M. T.; Plishka, M. J.; Robinson, K. D. *Metals in Biological Systems*; Ellis Horwood Limited: Chichester, 1992.
- (2) Ciardelli, F.; Tsuchida, E.; Wöhrl, D., Eds. *Macromolecule-Metal Complexes*; Springer-Verlag: Berlin, 1996.
- (3) Kaim, W.; Schwederski, B. *Bioinorganic Chemistry: Inorganic Elements in the Chemistry of Life*; John Wiley & Sons Ltd: Chichester, 1994.
- (4) Sigel, H.; Kapinos, L. E. *Coord. Chem. Rev.* **2000**, 200–202, 563.
- (5) Sigel, H.; Massoud, S. S.; Corfu, N. A. *J. Am. Chem. Soc.* **1994**, 116, 2958.
- (6) Sigel, H. *Chem. Soc. Rev.* **1993**, 22, 255.
- (7) Bianchi, E. M.; Sajadi, S. A. A.; Song, B.; Sigel, H. *Chem. Eur. J.* **2003**, 4, 881.
- (8) Herrero, L. A.; Terrón-Homar, A. *Inorg. Chim. Acta* **2002**, 339, 233.
- (9) Williams, N. H.; Takasaki, B.; Wall, M.; Chin, J. *Acc. Chem. Res.* **1999**, 32, 485.
- (10) Boraei, A.; Ibrahim, S. A.; Mohamed, A. H. *J. Chem. Eng. Data* **1999**, 44, 907.
- (11) Kiss, T.; Sóvágó, I.; Martin, R. B. *Inorg. Chem.* **1991**, 30, 2130.

- (12) Sawai, H.; Kuroda, K.; Hojo, T. *Bull. Chem. Soc. Jpn.* **1989**, 62, 2018.
- (13) Sawai, H.; Shibusawa, T.; Kuroda, K. *Bull. Chem. Soc. Jpn.* **1990**, 63, 1776.
- (14) Shimazu, M.; Shinozuka, K.; Sawai, H. *Angew. Chem., Int. Ed. Engl.* **1993**, 32, 870.
- (15) Sawai, H.; Katsutaka, H.; Kuroda, K. *J. Chem. Soc., Perkin Trans.* **1992**, 505.
- (16) Sawai, H.; Ito, T.; Kokaji, K.; Shimazu, M.; Shinozuka, K.; Taira, H. *Bioorg. Med. Chem. Lett.* **1996**, 6, 1785.
- (17) Sawai, H.; Hirano, A.; Mori, H.; Shinozuka, K.; Dong, B.; Silverman, R. H. *J. Med. Chem.* **2003**, 46, 4926.

tion of the uranyl ion as photochemical agent for cleavage of nucleic acids.<sup>18–23</sup> The uranyl ion,  $\text{UO}_2^{2+}$ , has two oxygen ligands, so-called “yl”-oxygens, that are chemically inert under most circumstances, while the exchangeable ligands are all located in a plane perpendicular to the linear  $\text{UO}_2$  unit. Hence, the steric requirements in ligand substitution reactions and in template and catalytic reactions are strict, one of the prerequisites for selectivity in these types of reactions. The  $\text{UO}_2^{2+}$  unit polarizes the coordinated ligands strongly and may enhance the nucleophilicity of a OH group of a sugar moiety and thereby organize the ligands by coordination to promote internucleotide bond formation from activated nucleotides. Hence, it can be a very effective catalyst in oligonucleotide synthesis.<sup>12</sup>

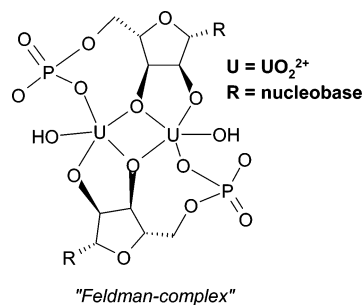
The “yl”-oxygens in the uranyl ion can be labilized in two ways, either by coordination of a strong Lewis base or by photochemical activation. The photoexcited uranyl ion is a strong oxidant for a variety of substrates, among others nucleic acids. The uranyl-mediated photocleavage is an important method to probe the tertiary structure of various nucleic acids and to identify metal ion binding sites in these ligands.<sup>21–23</sup>

Although the mechanism of these processes has not yet been fully elucidated, the coordination of the phosphate group to the uranyl ion and the coordination geometry of the formed complexes are of key importance in these reactions. A common observation for both processes<sup>12,23</sup> is that the reactions are practically absent above  $\text{pH} = 8.5$ , thereby indicating a dramatic change in the structure of the complexes. However, the structural changes, which result in the loss of the catalytic activity, are unknown. The main objective of this paper is to resolve these issues.

There are surprisingly few investigations dealing with the structure of uranium(VI)-nucleotide complexes in aqueous solutions.<sup>24–29</sup> The first study by Feldman and co-workers in the mid 1960s was initiated by the physiological role of the uranyl-adenosine triphosphate complex.<sup>24</sup> In their pioneering work,  $^1\text{H}$  NMR spectroscopy was used to suggest the formation of three complexes with AMP (adenosine-monophosphate) at  $\text{pH}$  above 8: one dimer with a uranium-to-ligand ratio of 2:2 and two other with the ratio 4:2.<sup>25</sup> One year later they reinvestigated and modified their originally proposed structure of the 2:2 dimer<sup>26</sup> to the one shown in Scheme 2.

This proposal served thereafter as a model for other metal-nucleotide complexes with, for example, molybdenum and was later cited as a “sandwich-type” or “Feldman complex”.<sup>30</sup> In the mid 1980s, two research groups reinvestigated the uranium-(VI) system, using  $^1\text{H}$  and  $^{31}\text{P}$  NMR spectroscopy. Both confirmed the formation of three uranium(VI)-AMP complexes, but one group reported<sup>28</sup> the same structures proposed by

Scheme 2



Feldman, while the other group<sup>29</sup> proposed the formation of two tetranuclear and one octanuclear complex with hydroxo bridges between the uranyl units. Even though the different structural proposals<sup>24–29</sup> are clearly in conflict with each other, they are uncritically used as models for the intermediates in both uranium(VI)-catalyzed reactions discussed above.

To find the correct structures and to decide how the complexes act in catalytic reactions, we reinvestigated the complex formation of uranium(VI) with four nucleotides in the alkaline  $\text{pH}$  range by multinuclear NMR spectroscopy.

## Experimental Section

**Sample Preparations.** The test solutions were prepared by adding a highly concentrated NaOD solution to a magnetically stirred suspension of the appropriate amount of the disodium salts of various nucleotides (Fluka) and  $\text{UO}_2(\text{NO}_3)_2 \cdot 6\text{H}_2\text{O}$  (Merck) in pure  $\text{D}_2\text{O}$  or  $\text{H}_2\text{O}$  (with 5%  $\text{D}_2\text{O}$ ) until the solutions became transparent (at around  $\text{pH} = 8.5$ ). The  $\text{pH}$  of the solution was then increased by NaOD to reach the desired  $\text{pH}$  between 8.5 and 12 for the NMR samples (see also eq 1 below for  $[\text{H}^+]$  balance). The  $\text{pD}$  in pure  $\text{D}_2\text{O}$  solvent was calculated from glass electrode measurements using  $\text{pD} = \text{pH} + 0.4$ .<sup>31</sup> The samples could be kept for several weeks in daylight at room temperature without any sign of hydrolysis or photochemical decomposition of the complexes.

**NMR Measurements.** The NMR spectra were recorded on a Bruker DMX500 spectrometer at  $25^\circ\text{C}$ , either in  $\text{D}_2\text{O}$  or in  $\text{H}_2\text{O}$  (with 5%  $\text{D}_2\text{O}$  in the latter to obtain a locked mode), equipped with 5 mm inverse (for  $^1\text{H}$ ) and 5 or 10 mm normal (for  $^{17}\text{O}$ ,  $^{31}\text{P}$ , and  $^{13}\text{C}$ ) NMR probe heads. The  $^1\text{H}$  and  $^{13}\text{C}$  NMR spectra (recorded at 500.1 and 125.7 MHz, respectively) are referenced to the methyl signal of external TMS, the  $^{17}\text{O}$  ones (67.8 MHz) to water at  $25^\circ\text{C}$ , and the  $^{31}\text{P}$  ones (202.4 MHz) to 85%  $\text{H}_3\text{PO}_4$  at  $25^\circ\text{C}$ .  $^{17}\text{O}$  NMR measurements were performed using  $^{17}\text{O}$ -enriched samples. The  $^{17}\text{O}$ -enrichment of the “-yl” oxygens of the uranyl ion was accomplished by a procedure described previously.<sup>32</sup> For the quantitative evaluation of the integrals in the proton-decoupled  $^{31}\text{P}$  spectra these were measured by inverse-gated decoupling. The stoichiometry of the complexes is based on the integral values of the  $^1\text{H}$  and  $^{31}\text{P}$  NMR signals of the coordinated and free ligands and the  $^{17}\text{O}$  NMR signals of the coordinated uranyl ions. These were measured at different uranium(VI) and nucleotide concentrations in the  $\text{pH}$  range of 8.5–12.

The diffusion experiments were performed on a Bruker DMX200 spectrometer equipped with a wide-bore Bruker gradient probe with a maximum gradient of  $9.6\text{ T m}^{-1}$ . Pulsed-field-gradient stimulated-echo  $^1\text{H}$  NMR experiments recorded the variation of individual peak intensities in the  $^1\text{H}$  spectrum upon increasing the gradient strength (up to  $1.2\text{ T m}^{-1}$ ). The self-diffusion coefficients corresponding to individual spectral peaks were extracted by fitting the conventional Stejskal–Tanner expression<sup>33</sup> to these data. The random error in the

(18) Nielsen, P. E.; Jeppesen, C.; Buchardt, O. *FEBS Lett.* **1988**, *235*, 122.

(19) Hill, A. R., Jr.; Orgel, L. E. *Bioconjugate Chem.* **1991**, *2*, 431.

(20) Nielsen, P. E.; Hiort, C.; Sönnichsen, S. H.; Buchardt, O.; Dahl, O.; Nordén, B. *J. Am. Chem. Soc.* **1992**, *114*, 4967.

(21) Nielsen, P. E.; Møllegaard, N. E. *J. Mol. Recognit.* **1996**, *9*, 228.

(22) Sönnichsen, S. H.; Nielsen, P. E. *J. Mol. Recognit.* **1996**, *9*, 219.

(23) Wittberger, D.; Berens, C.; Hammann, C.; Westhof, E.; Schroeder, R. *J. Mol. Biol.* **2000**, *300*, 339.

(24) Feldman I.; Jones, J.; Cross, R. *J. Am. Chem. Soc.* **1967**, *89*, 49.

(25) Agarwal, R. P.; Feldman, I. *J. Am. Chem. Soc.* **1968**, *90*, 6635.

(26) Feldman I.; Rich, K. E. *J. Am. Chem. Soc.* **1969**, *91*, 4559.

(27) Rich, K. E.; Agarwal, R. P.; Feldman I. *J. Am. Chem. Soc.* **1970**, *92*, 6818.

(28) Castro, M. M. C. A.; Geraldles, C. F. G. C. *Inorg. Chim. Acta* **1987**, *140*, 377.

(29) Kainosho, M.; Takahashi, M. *Nucl. Acid Res. Symp. Ser.* **1983**, *12*, 181.

(30) Geraldles, C. F. G. C.; Castro, M. M. C. A. *J. Inorg. Biochem.* **1986**, *28*, 319.

(31) Glasoe, P. K.; Long, F. A. *J. Phys. Chem.* **1960**, *64*, 188.

(32) Bányai, I.; Glaser, J.; Micskei, K.; Tóth, I.; Zékány, L. *Inorg. Chem.* **1995**, *34*, 3785.

obtained diffusion coefficients is estimated to be less than 3%. The absolute value of the obtained diffusion coefficients was obtained by referencing the nominal diffusion data to the diffusion coefficient of water ( $D = 2.0 \text{ m}^2 \text{ s}^{-1}$  at  $21^\circ \text{C}$ ) measured under identical conditions.

**Crystallography.** The yellow needle-shaped crystals were formed after a couple of weeks at room temperature in the closed solutions of the binary uranium(VI)-AMP system above pH 10. Since the selected single crystals decomposed within a few hours in air, even at low temperature (173 K) coated by epoxy glue, a new crystal was put in a capillary together with a drop of mother liquor, for the diffraction experiment. The X-ray intensity data were collected using a STOE IPDS (Imaging Plate Diffraction System) instrument, equipped with a rotating anode.<sup>34</sup> Data reduction calculations included corrections for background, Lorentz, polarization, and absorption effects.<sup>34,35</sup> In the numerical absorption corrections the transmission factors (T) was assumed to vary between 17.9 and 63.9%.

The crystallographic unit cell has an almost perfect hexagonal shape. Nevertheless, inspection of the reflection intensities clearly indicated that the structure has no exact hexagonal symmetry. Despite of the 3-fold rotational molecular symmetry of each of the trimeric complex units, no crystallographic symmetry at all could be detected in the observed diffraction pattern. Hence, the structure was solved assuming the triclinic enantiomorphous space group  $P1$  with  $Z = 1$ . Accordingly, the unique part of the structure is equal to the whole unit cell content,  $\text{C}_{60}\text{H}_{126}\text{N}_{30}\text{O}_{89}\text{Na}_{8.5}\text{P}_6\text{U}_6$ , i.e., about 200 non-hydrogen atoms. The formula  $\text{C}_{60}\text{H}_{126}\text{N}_{30}\text{O}_{89}\text{Na}_{8.5}\text{P}_6\text{U}_6$  has been deduced from the results of the X-ray structure analysis. Furthermore, some of the sodium counterions [Na(7)–Na(12)] as well as some of the water oxygens [O(11W), O(21W), O(41W), O(51W), O(52W), O(71W), O(72W), and O(1WP)–O(6WP)] exhibit not only dynamic but also static disorder, the latter indicated by their partial site occupation factors (sof's). The hydrogen atoms of the complex units have been located in positions that were calculated using geometric evidence,<sup>36</sup> whereas the water H atoms, belonging to the interstitial, more or less disordered water O atoms, are not included in the final structure model. Refinement of the large number of atoms and their variables required a huge memory version of the SHELXL program (SHELXH).<sup>36</sup> The refinement calculations seem to support the low-symmetry space group ( $P1$ ), although a few correlation coefficients larger than 0.5 have been detected in the course of the least-squares calculations, suggesting the presence of approximate (pseudo) crystal symmetry. The Flack asymmetry parameter,  $x$ ,<sup>36,37</sup> converged to the relatively low value of  $-0.001(7)$ , hence indicating that the absolute structure has been determined reliably. Accordingly, the final atomic coordinates as well as the crystallographic illustrations of the complex refer to the correct absolute structure. Crystal data, together with further details of the data reduction and refinement calculations, are shown in Table 1.

Crystallographic numbering of the core atoms is given in the Supporting Information, Figure S1a,b.

## Results and Discussion

The complex formation of uranium(VI) in binary and ternary uranium(VI)-nucleotide systems has been studied using four nucleotides, adenosine- (AMP), guanosine- (GMP), uridine- (UMP), and cytidine-monophosphate (CMP). Our conclusions on the structure and constitution of the complexes can be summarized as follows.

(i) Only two complexes are formed in the investigated pH region independently of the total uranium(VI) and ligand concentrations and of ligand type.

**Table 1.** Crystal Data and Details of the Data Reduction and Final Refinement Calculations for *Complex-II*

chemical formula sum	$\text{C}_{60}\text{H}_{126}\text{N}_{30}\text{O}_{89}\text{Na}_{8.5}\text{P}_6\text{U}_6$
fw	4501.32
temperature, K	293(2)
radiation/ $\lambda$ , Å	Mo K $\alpha$ /0.71073
cryst syst/space group	triclinic/ $P1$
unit cell dimens	
$a$ , Å	8.4610(10)
$b$ , Å	26.688(4)
$c$ , Å	26.690(4)
$\alpha$ , deg	60.03(2)
$\beta$ , deg	89.98(2)
$\gamma$ , deg	89.78(2)
$V$ , Å <sup>3</sup>	5220.8(13)
$Z$	1
$D_c$ , Mg m <sup>-3</sup>	1.432
$\mu$ , mm <sup>-1</sup>	4.78
$F(000)$	2144
approximate cryst size, mm	$0.30 \times 0.19 \times 0.11$
$\theta_{\text{max}}$ for collected data, deg	23.99
index ranges min./max. $h,k,l$	$-8/9, -30/30, -30/30$
no. of refls collected	29 702
no. of indep refls	25 871
$R_{\text{int}}$	0.0636
refinement method	full-matrix least-squares on $F^2$
no. of parameters refined	1899
$R(F)$ (all $F$ values)	0.054
$R(F)$ [ $I > 2\sigma(I)$ ]	0.044
no. of refls with $I > 2\sigma(I)$	22 429
$wR(F)^2$ (all $F^2$ values)	0.117
goodness-of-fit on $F^2$	1.029
mean/max. values of final shift/esd	0.000/0.001
largest diff peak and hole, e <sup>-</sup> Å <sup>-3</sup>	1.02 and $-0.90$

<sup>a</sup> The weights of the  $F^2$  values were assumed as  $w = [\sigma^2(F^2) + (c_1P)^2 + (c_2P)]^{-1}$ , where  $P = (F_o^2 + 2F_c^2)/3$ , and the constants  $c_1$  and  $c_2$  had the values 0.0745 and 0.000.

(ii) Although the 5'-phosphate group and the 2'- and 3'-hydroxyl groups of the sugar unit are coordinated to the uranyl ions in a way similar to that in the originally suggested "Feldman complex" (Scheme 2), the structures of the complexes are different from those previously suggested, with the metal-to-ligand ratio of 6:4 in one of the complexes and 3:3 in the other one.

Our proposals for the structure of the complexes are shown in Scheme 3 (I and II). These are based on the results of various NMR experiments (integral values, chemical shifts, homo- and heteronuclear couplings, diffusion coefficients) and also confirmed by two-dimensional (2D) homo- and heteronuclear correlation spectra (Supporting Information, Figure S2a–f) as discussed below.

**The Number of Distinct Complexes.** The <sup>1</sup>H NMR spectra measured in various uranium(VI)-nucleotide systems, in the pH range of 8.5 and 12, show three signals for each hydrogen in the coordinated ligands in addition to the signals of the free nucleotide. In accordance with this, three signals can be observed for the coordinated nucleotides in the corresponding <sup>31</sup>P NMR spectra (Figure 1).

The intensities of two of these signals are always identical independently of the total ligand and metal concentrations. They also decrease with the pH, while the intensity of the third signal increases, as can be seen in the <sup>1</sup>H and <sup>31</sup>P spectra measured in the AMP system (Figures 2 and 3).

In earlier studies, the signals with identical intensities were assigned to two different species with the same thermodynamic stability.<sup>26,28,29</sup> Instead, we claim that these signals belong to the same complex (for simplicity referred to as *Complex-I* in the following).

(33) Stejskal, E. O.; Tanner, J. E. *J. Chem. Phys.* **1965**, *42*, 288.

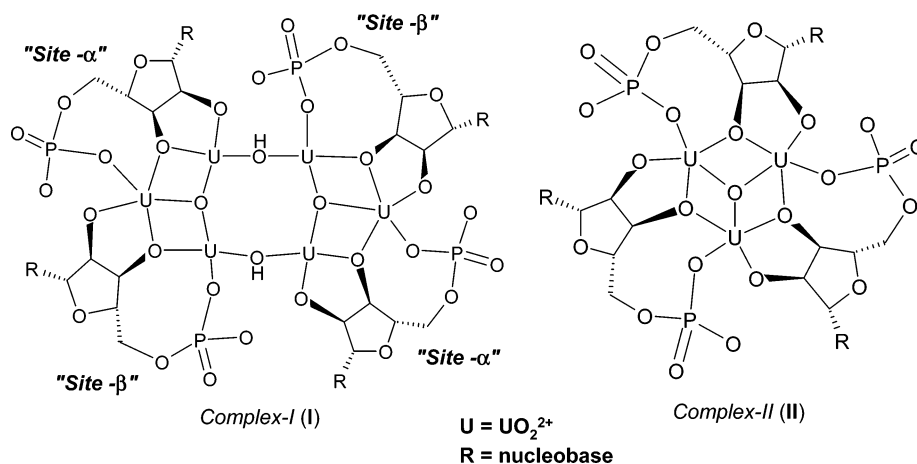
(34) STOE & CIE GmbH, 1997 (Publications 4805–4816).

(35) *X-Shape and X-Red*; STOE & CIE GmbH: Darmstadt, Germany, 1997.

(36) Sheldrick, G. M. *SHELXH, a huge memory version of SHELXL-97*; University of Göttingen: Germany, 1997.

(37) Flack, H. D. *Acta Crystallogr.* **1983**, *A39*, 876–881.

Scheme 3



As shown in Table 2, the diffusion data obtained for two of the  $^1\text{H}$  lines within the H-8 and H-1' groups coincide within experimental error of 3% (see assignments in Table 4).

Note that the diffusion coefficient is a molecular property and therefore must be identical irrespective of which peak within the same molecule or complex is used for the measurement; hence, for example, corresponding diffusion coefficients for the H-8 and H-1' manifolds also coincide within experimental error. This result indicates that the two (set of) lines with identical intensity belong to entities of the same hydrodynamic radius. Hence, the spectral behavior (identical concentration of the entities to which the lines can be assigned), the chemical "constancy" (the two lines are of identical intensity irrespective of which nucleotide is the ligand), and the diffusion data (identical size for the entities) together prove beyond reasonable doubt that the two (set of) lines belong to the same complex but to two chemically distinct sites within *Complex-I*. These

will be referred to as "Site- $\alpha$ " and "Site- $\beta$ " in the following. The diffusion value for the third H-8 and H-1' signal pair is larger, which indicates that this complex (hereafter referred to as *Complex-II*) is smaller than *Complex-I*.

On the basis of the integrals of the  $^1\text{H}$  and  $^{31}\text{P}$  signals of the coordinated and the free ligands and the integrals of  $^{17}\text{O}$  signals for the coordinated uranyl ions, a 1:1 uranium-to-nucleotide ratio can be calculated for *Complex-II*. This value is in agreement with the earlier proposal (see Scheme 2 for the "Feldman complex"). However, the uranium-to-nucleotide ratio for *Complex-I* is 3:2 instead of 4:2, as was reported earlier. The difference can be explained as follows. Inversion recovery measurements showed that the spin-lattice ( $T_1$ ) relaxation times of the  $^{31}\text{P}$  and  $^1\text{H}$  signals in the coordinated ligands differ significantly from the corresponding signals in the free ligand. The  $^{31}\text{P}$  spin-lattice relaxation is faster and the  $^1\text{H}$  relaxation is slower in the coordinated nucleotides than in the free ligand. The relaxation times are also different between the corresponding signals of the two coordinated ligands in *Complex-I*. Hence, care must be taken while recording the spectra, since the intensity of the signals is strongly dependent on the relaxation delay; if this is not long enough, the metal-to-ligand ratio calculated from the integrals will be in error. According to our observations, the relaxation delay must be at least 5 s for the  $^{31}\text{P}$  and 10 s for the  $^1\text{H}$  experiments in order to obtain proper integral values. We assume that this may not have been fulfilled in these earlier studies.

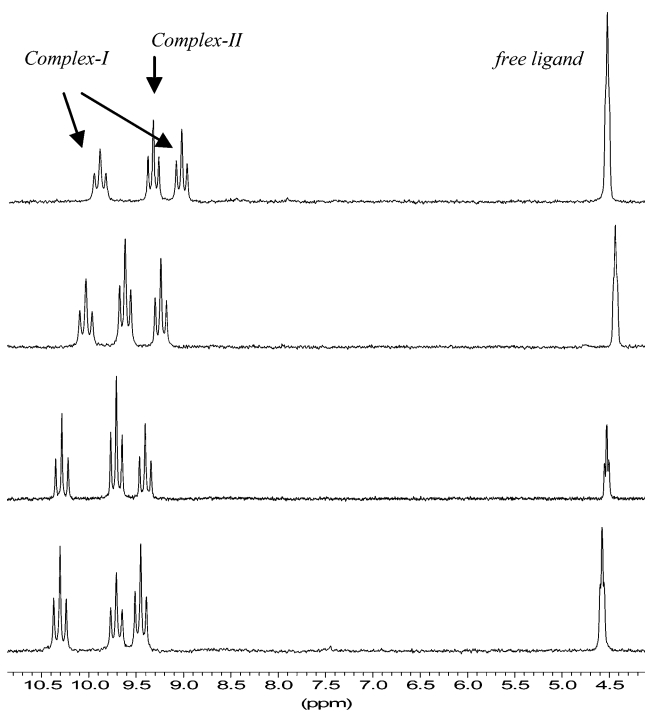


**Figure 1.**  $^{31}\text{P}$  NMR spectra measured in the binary U(VI)-nucleotide systems at 50 mM uranium(VI) and 50 mM nucleotide concentrations at pH = 9.5. Nucleotides are, from bottom to top, AMP, GMP, CMP, and UMP.

**Combinatorial Approach of the Constitution of the Formed Complexes.** In general the variation of the pH and/or the ratio of the concentration of the metal and ligand provide information about the composition of the complexes formed. However, this is not the case in systems where multinuclear, symmetric complexes are formed; for example, the metal-to-ligand ratio of 1:1 may correspond to a stoichiometry of 2:2; 3:3, and so on. The proper stoichiometry can then be obtained by using a mixture of two different nucleotides. In this case structural isomers with different NMR signals can be formed, from which the number of coordinated ligands can be deduced. Kainosho et al.<sup>29</sup> used an equimolar mixture of AMP and CMP and observed four signals for the H-1' AMP-ribose protons in the assumed structure of the "Feldman complex". From this, they erroneously concluded that this is an octanuclear complex. On the basis of the same results they also proposed the formation of two tetranuclear complexes.

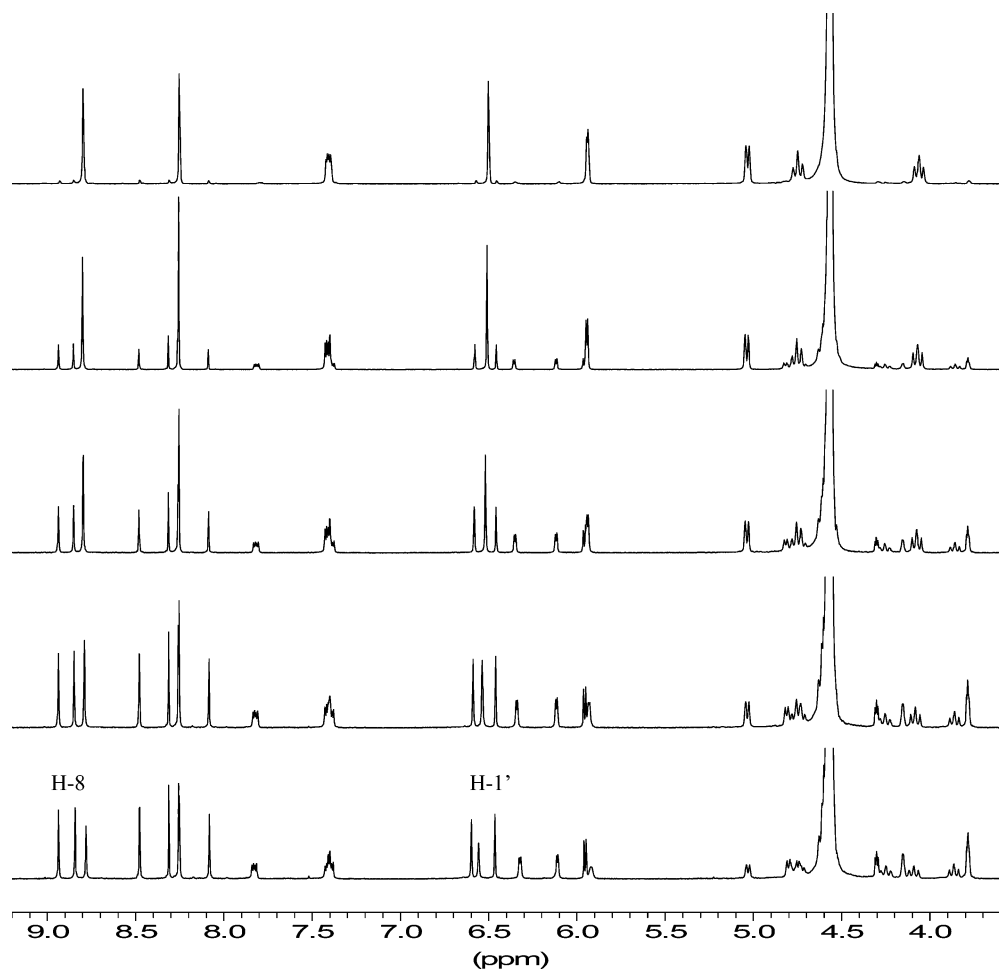


**Figure 2.** pH dependence of the  $^1\text{H}$  NMR spectra measured in the binary U(VI)-AMP system ( $[\text{UO}_2^{2+}] = 52 \text{ mM}$ ,  $[\text{AMP}] = 53 \text{ mM}$ ). pH from bottom to top: 9.44, 9.68, 10.15, 10.58, and 11.60. The sets of H-8 and H-1' proton signals used in the diffusion measurements are marked in the bottom spectrum. The full assignment of the signals is given in Table 4.

To resolve these issues, we have recorded multinuclear NMR spectra in various ternary systems using mixtures of two nucleotides. We have found that the proton-decoupled  $^{31}\text{P}$  NMR spectra are the most informative in these systems to deduce the number of coordinated ligands, because the chemical shift differences between the phosphorus signals of coordinated ligands in the various complexes are larger than those for the corresponding proton signals. The proton-decoupled  $^{31}\text{P}$  NMR spectrum measured at a total concentrations of 50 mM of uranium(VI), 25 mM of AMP, and 25 mM of CMP is shown in Figure 4b.

On the basis of this type of experiments the following conclusions can be drawn on the constitution of the complexes.

**Complex-II.** The single  $^{31}\text{P}$  signal measured in the binary systems for *Complex-II* with 1:1 uranium(VI)-AMP ratio indicates that any number of coordinated ligands must be in symmetric positions (Figure 4a).

If only two ligands are coordinated, as was proposed by Feldman (see Scheme 2), then three different complexes should be formed in the ternary system obtained using a mixture of AMP (A) and CMP (C); these ligand combinations result in the complexes AA, AC (=CA), and CC. Using an equimolar mixture of the ligands and assuming the same thermodynamic stabilities of the complexes, the ratio of the relative population of the complexes would be 1:2:1 (AA:AC(=CA):CC). For AA and CC only one signal (one for A and one for C) could be

detected due to their symmetry. One should note that the AC (=CA) complexes will give two  $^{31}\text{P}$  signals, one for each ligand. Consequently, the “Feldman complex” would result in two sets of two peaks, two for A and two for C with equal intensity. However, this is inconsistent with our results because two sets of signals are observed in the proton-decoupled  $^{31}\text{P}$  spectra, each consisting of four lines with equal intensities, as can be seen in Figure 4c.

Assuming that the number of ligands is three and keeping in mind their symmetric arrangement in the coordination sphere, a quasi-linear structure of the complexes with a 1:1 metal-to-ligand ratio can be excluded. In a cyclic arrangement of the ligands, there are eight possibilities, as shown in Scheme 4. For equimolar mixtures, the relative ratio of the complexes is AAA(a) = 1, AAC(b,c,d) = 3, ACC(f,g,h) = 3, and CCC(e) = 1. In AAA (or CCC) the three ligands are equivalent and have one  $^{31}\text{P}$  signal ( $A_1$  and  $C_1$ ), respectively. In AAC there are two different phosphorus sites for AMP,  $A_2$  (where the phosphate group is adjacent to the nucleobase in  $A_3$ ) and  $A_3$  (where the phosphate group is adjacent to the nucleobase in  $C_4$ ), and one site for CMP,  $C_4$  (where the phosphate group is adjacent to the nucleobase in  $A_2$ ), as indicated in Scheme 4. In ACC, in a similar manner, there are two different phosphorus sites for CMP ( $C_2$  and  $C_3$ ) and one for AMP ( $A_4$ ). Hence, four signals should be observed for each ligand,  $A_1, A_2, A_3, A_4$  and  $C_1, C_2, C_3, C_4$ , respectively. Taking into account the populations

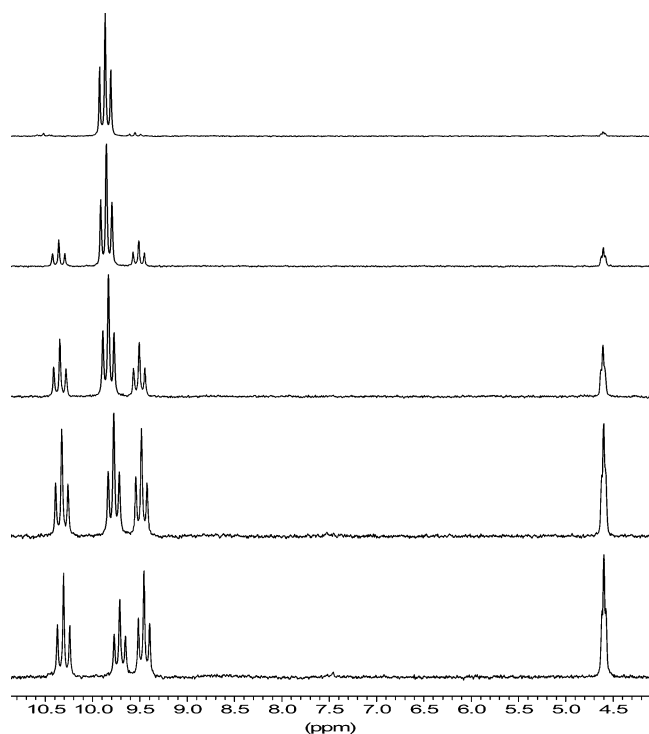


**Figure 3.** pH dependence of the  $^{31}\text{P}$  NMR spectra measured in the binary uranium(VI)-AMP system ( $[\text{UO}_2^{2+}] = 52 \text{ mM}$ ,  $[\text{AMP}] = 53 \text{ mM}$ ). pH from bottom to top: 9.44, 9.68, 10.15, 10.58, and 11.60. The assignments of the signals are given in Figure 1.

of the complexes, it is easy to see that the intensities of the signals are equal, as observed in our spectra (Figure 4c). This confirms unambiguously the coordination of three nucleotides in *Complex-II* and not two or eight as was proposed earlier. The identical intensity of the AMP and CMP signals also confirms that the involved isomers (Scheme 4) have similar thermodynamic stabilities.

**Complex-I.** As mentioned before the two  $^{31}\text{P}$  signals measured in the binary system indicate that there are two different coordination sites in *Complex-I*, as shown in Figure 4a. Using an equimolar mixture of AMP and CMP four sets of four  $^{31}\text{P}$  signals, altogether 16 signals, are observed for “*Site- $\alpha$* ”, which are shown in Figure 4c. As one can see in the same figure, four groups of signals can also be observed for “*Site- $\beta$* ”; however, the peaks within those groups are less resolved than those for “*Site- $\alpha$* ”. This can be explained by a chemical shift at this site that is less sensitive for the coordination geometry, as discussed later. This large number of  $^{31}\text{P}$  signals indicates that the number of coordinated ligands in this complex must be larger than two. Hence, taking into account the metal-to-ligand ratio of 3:2 calculated previously, we can assume that the ligand ratio has the next highest integer value 6:4, that is, four nucleotides coordinated to six uranium atoms. The coordination of the ligands must be symmetric in such a way that two of them are located in site “*Site- $\alpha$* ” and two in “*Site- $\beta$* ”; hence a quasi-linear arrangement of the ligands can be excluded. Using these assumptions, the combination of the ligands results in the formation of 16 complexes in a mixture of two nucleotides, which can be seen in Table 3 and, in more detail, in the Supporting Information, Figure S3. Six pairs of them are identical, thereby creating 10 different ligand combinations, as illustrated in the first two columns of Table 3.

For simplicity the letters on the edges of the complex assignment correspond to “*Site- $\alpha$* ”, while those in the middle correspond to “*Site- $\beta$* ”. Using an equal amount of the two nucleotides the intensities of the  $^{31}\text{P}$  signals of the complexes are approximately the same, as can be seen in Figures 4c and 5c. On this basis, we can state that the thermodynamic stability of the complexes formed in the ternary systems is approximately the same and independent from the nucleotide.

To definitively prove the 6:4 coordination, we have recorded spectra at AMP to CMP ratios of approximately 1:2.5 and 2:1, which showed characteristic changes of signal intensities (Figure 5a,b).

The relative populations of the complexes calculated at 2:1 AMP to CMP ratio and the calculated (on the basis of 6:4 coordination) and measured relative  $^{31}\text{P}$  signal intensities of AMP and CMP ligands coordinated in “*Site- $\alpha$* ” are given in Table 3. The relative populations of complexes can be calculated by simple multiplication of relative ligand concentrations. To calculate the intensities of the  $^{31}\text{P}$  signals, the symmetry of the different molecules must also be considered. For example, in the symmetric *AAAA* molecule, the two AMP ligands in “*Site- $\alpha$* ” (marked by *italic* letters) are equivalent. In these the phosphate groups are adjacent to the nucleobase of the AMPs in “*Site- $\beta$* ”; hence, they show one signal whose relative intensity is just twice that of the relative population of this complex, which is 32. However, in *AACA* the two AMP ligands in “*Site- $\alpha$* ” are not equivalent (in one the phosphate group is adjacent to the nucleobase of AMP, while in the other it is adjacent to the nucleobase of CMP in “*Site- $\beta$* ”), and therefore each has a different signal. Considering the relative population of this isomer ( $2 \times 8$ , i.e., 16), the relative intensity of each signal is 16. In this way the relative intensities for all signals in “*Site- $\alpha$* ” can be calculated and compared with those from the deconvolution of the measured peaks in Figure 5b. One can see that the calculated and experimental values are in excellent agreement for “*Site- $\alpha$* ” (see Table 3). Hence, we can conclude that there are four coordinated ligands in *Complex-I*. It is worth recalling that the ratio of the diffusion coefficients (see Table 2) for *Complex-II* and *Complex-I* is about 1.2. This shows, in accordance with our deduced structures, that *Complex-I* must be the larger one. The relative change in hydrodynamics radius correlates well with the 4:3 ratio of ligands involved in the two complexes.

On the basis of the comparison of the measured and the calculated intensities in Table 3, the signals can be assigned to the corresponding complexes. The first eight signals with higher chemical shifts belong to the AMP ligands, while the other eight signals belong to the CMP molecules. These signals are still separated into two groups in which the orders and relative intensities (in parentheses) measured at 2:1 AMP to CMP ratio are the following: for AMP, *AAAA* (32), *AAAC* (16), *AACA* (16), *AACC* (8) and *ACAA* (16), *ACAC* (8), *ACCA* (8), *ACCC* (4); for CMP, *CAAA* (16), *CAAC* (8), *CACA* (8), *CACC* (4) and *CCAA* (8), *CCAC* (4), *CCCA* (4), *CCCC* (2). This order of chemical shifts will be discussed in the next paragraph in relation to the structure of the complexes.

**Structure of the Complexes.** The most characteristic spectral parameters that support our suggested structure of the complexes are discussed here. To begin, it is worth mentioning that the most common coordination geometry of uranium(VI) complexes

**Table 2.** Self-Diffusion Data, Corrected to Water Diffusion

peak	H-8			H-1'		
	Complex-I		Complex-II	Complex-I		Complex-II
	"Site- $\alpha$ "	"Site- $\beta$ "		"Site- $\alpha$ "	"Site- $\beta$ "	
$D$ ( $10^{-10}$ m $^2$ s $^{-1}$ )	1.65 $\pm$ 0.03	1.67 $\pm$ 0.03	2.06 $\pm$ 0.04	1.73 $\pm$ 0.04	1.70 $\pm$ 0.04	2.03 $\pm$ 0.04

<sup>a</sup> The diffusion coefficient of free AMP monomers was obtained as  $3.45 \times 10^{-10}$  m $^2$  s $^{-1}$ .

**Table 3.** Combinatorial Assignments of the Relative Population of the Isomers for *Complex-I* (formed in the ternary uranium(VI)-AMP-CMP system using a 2:1 AMP:CMP ratio) and the Calculated and Measured (in parantheses) Relative  $^{31}\text{P}$  NMR Signal Intensities for "Site- $\alpha$ " (see details in the text)

complex ( $S_{\alpha}, S_{\beta}, S_{\gamma}, S_{\delta}$ )	no. of identical isomers ( $N$ )	relative population of the isomers ( $P$ )	$(N) \times (P)$	calcd and measd relative $^{31}\text{P}$ NMR signal intensities for <i>Complex-I</i> in "Site- $\alpha$ "	
				for <b>A</b> (AMP)	for <b>C</b> (CMP)
AAAA	1	16 ( $2 \times 2 \times 2 \times 2$ )	16	32 = $2 \times 16$ ; (28.5)	0
AAAC (CAAA)	2	8 ( $2 \times 2 \times 2 \times 1$ )	16	16 (21)	16 (14.5)
ACA (ACAA)	2	8 ( $2 \times 2 \times 1 \times 2$ )	16	16 + 16 (16 <sup>a</sup> + 16.4)	0
AACC (CCAA)	2	4 ( $2 \times 2 \times 1 \times 1$ )	8	8 (9.2)	8
ACAC (CACA)	2	4 ( $2 \times 1 \times 2 \times 1$ )	8	8 (8.8)	8 (8.3)
ACCA	1	4 ( $2 \times 1 \times 1 \times 2$ )	4	8 = $2 \times 4$ ; (8.3)	0
ACCC (CCCA)	2	2 ( $2 \times 1 \times 1 \times 1$ )	4	4 (4.2)	4 (5.5)
CCCC	1	1 ( $1 \times 1 \times 1 \times 1$ )	1	0	2 = $2 \times 1$ ; (2.5)
CAAC	1	4 ( $1 \times 2 \times 2 \times 1$ )	4	0	8 = $2 \times 4$ ; (8.8)
CACC (CCAC)	2	2 ( $1 \times 2 \times 1 \times 1$ )	4	0	4 + 4 (4.8 + 4.5)

<sup>a</sup> The intensities of the deconvoluted peaks are calibrated to the relative intensity of 16 for this peak (AMP signal from AAAC, third peak from the left in Figure 5b).

**Table 4.**  $^1\text{H}$ ,  $^{13}\text{C}$ , and  $^{31}\text{P}$  NMR Chemical Shifts (measured in D $_2$ O at 25 °C) for Free AMP and the Complexes in the Binary Uranium(IV)-AMP System<sup>a</sup>

nucleus		chemical shift ( $\delta$ ) in ppm			
		free AMP	Complex-I		Complex-II
		"Site- $\alpha$ "	"Site- $\beta$ "		
$^1\text{H}$	H-1'	5.98	6.64 (0.66)	6.52 (0.54)	6.56 (0.65)
	H-2'	4.68 <sup>b</sup>	<b>6.40 (1.72)</b>	<b>6.18 (1.50)</b>	<b>6.00 (1.32)</b>
	H-3'	4.39	<b>7.85 (3.45)</b>	<b>7.42 (3.03)</b>	<b>7.44 (3.05)</b>
	H-4'	4.24	4.87 (0.63)	4.70 <sup>b</sup> (0.46)	5.12 (0.88)
	H-5'	3.89	<b>4.80 (0.91)</b> , 4.35 (0.46)	<b>4.70<sup>b</sup> (0.81)</b> , 3.97 (0.08)	<b>4.85 (0.96)</b> , 4.17 (0.28)
$^{13}\text{C}$	H-2	8.06	8.35 (0.29)	8.30 (0.24)	8.27 (0.21)
	H-8	8.46	8.95 (0.49)	8.86 (0.40)	8.80 (0.34)
	C-1'	86.80	90.95 (4.15)	90.95 (4.15)	90.78 (3.98)
	C-2'	74.40	<b>90.25 (15.85)</b>	<b>89.58 (15.18)</b>	<b>88.73 (14.33)</b>
	C-3'	70.60	<b>87.50 (16.9)</b>	<b>84.81 (14.21)</b>	<b>84.26 (13.66)</b>
	C-4'	84.60	83.41 (-1.19)	83.57 (-1.03)	84.26 (-0.34)
	C-5'	63.39	65.32 (1.93)	62.94 (-0.45)	62.77 (-0.62)
	C-2	152.63	152.77 (0.14)	152.69 (0.06)	152.69 (0.06)
$^{31}\text{P}$	C-4	148.80	148.73 (-0.07)	148.50 (-0.3)	148.58 (-0.22)
	C-5	118.33	118.83 (0.50)	118.59 (0.26)	118.59 (0.26)
	C-6	155.32	155.54 (0.22)	155.45 (0.13)	155.45 (0.13)
	C-8	140.02	140.19 (0.17)	140.40 (0.38)	140.40 (0.38)
		4.6	10.3–10.4 <sup>c</sup>	9.45–9.55 <sup>c</sup>	9.7–9.9 <sup>c</sup>

<sup>a</sup> The numbers in parentheses indicate the chemical shift differences between the corresponding signals of the complexes and the free ligand.  
<sup>b</sup> Signals are overlapping with the solvent signal. <sup>c</sup> The values are changing with pH.

is a pentagonal bipyramid, with all labile ligands in the plane perpendicular to the linear UO $_2$  unit with some exceptions for four- and six-coordination. The tetragonal bipyramid geometry

is rare; the UO $_2(\text{OH})_4^{2-}$  complex is one example identified by EXAFS in solution.<sup>38</sup> Six-coordination is found for chelating ligands with a short ligand bite, such as carbonate and acetate or in some macrocyclic ligands.

**1.  $^1\text{H}$  and  $^{13}\text{C}$  NMR Spectra.** The very large similarities between the spectra measured with different nucleotides and the apparently identical thermodynamic stability of the complexes indicate identical structures where the nucleobase is not coordinated, irrespective of nucleotide. The full assignments of the  $^1\text{H}$ ,  $^{13}\text{C}$ , and  $^{31}\text{P}$  signals of the free and the coordinated AMP in both complexes are given Table 4.

As can be seen, most of the  $^1\text{H}$  and the  $^{13}\text{C}$  NMR signals appear with much higher chemical shift in the coordinated ligands in both complexes than in the free ligand. Particularly large chemical shift differences can be observed for the H-2', H-3', and in one of the H-5' methylene protons, as well as for C-2' and C-3' carbons upon coordination. (Boldfaced figures in Table 4.) The H-5' protons are coupled to one another and to the phosphorus atom: their chemical shift difference and coupling pattern (Figure S2c) indicate the formation of a rigid ring system. Our suggestion for the structure and site assignment of the complexes is given in Scheme 3. However, one has to note that two other symmetric structures can be drawn for *Complex-II* (see Supporting Information Figure S4, structures **III** and **IV**) beside the structure (**II**) given in Scheme 3. These differ only in the bridging atom; in one of the structures (**III**)

(38) Clark, D. L.; Conradson, S. D.; Donohoe, R. J.; Keogh, R. J.; Morris, D. E.; Palmer, P. D.; Rogers, R. D.; Tait, C. D. *Inorg. Chem.* **1999**, *38*, 1456.



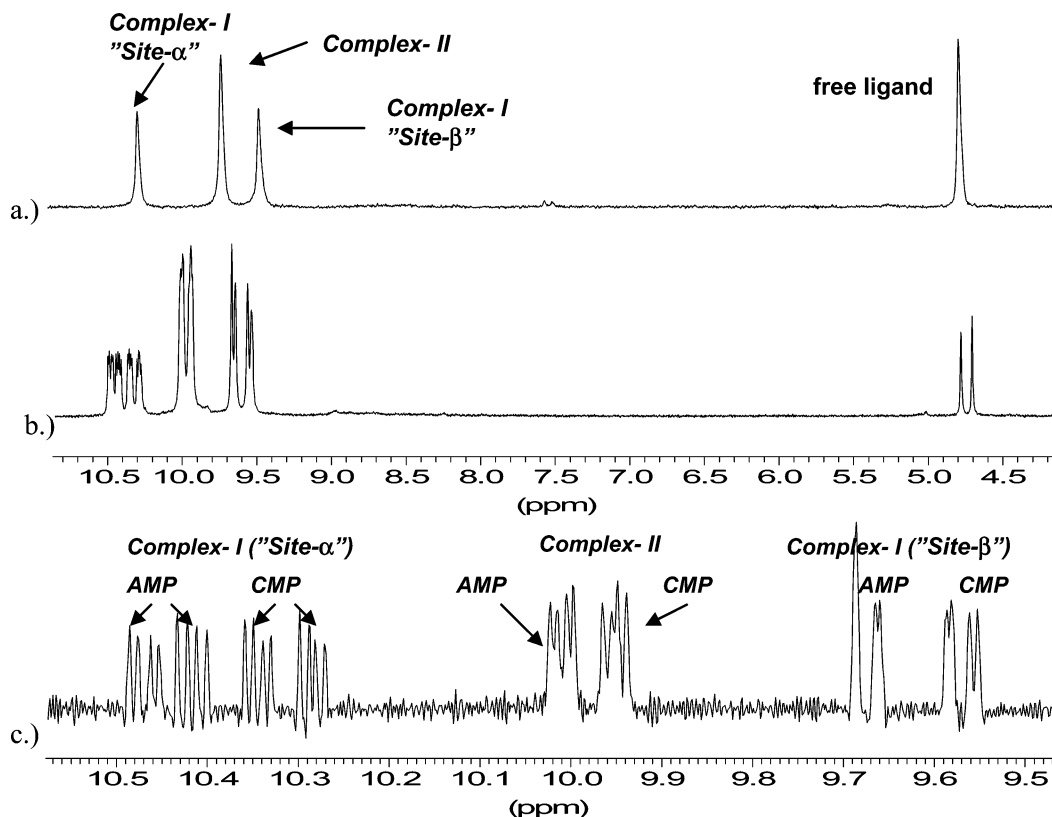
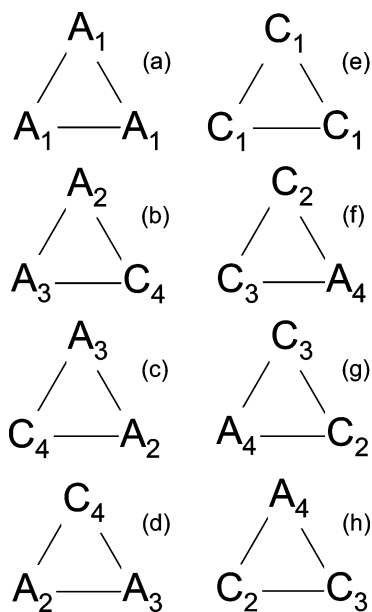


**Figure 4.** Proton-decoupled  $^{31}\text{P}$  NMR spectra measured in the binary uranium(VI) (50 mM)-AMP (50 mM) (a) and the ternary uranium(VI) (50 mM)-AMP (25 mM)-CMP (25 mM) systems (b) at pH = 9.4, and a resolution-enhanced inset of the signals of the complexes in the latter spectrum (c).

#### Scheme 4



the 2'-OH oxygen and in the other (IV) one of the phosphate oxygens is in the bridge position between two uranyl ions. However, taking into account the 2–3 times larger highfield shift of the H-3' proton compared to those of the H-2' or H-5' protons, we suggest that the 3'-hydroxide is in a bridge position in both complexes, as shown in Scheme 3. It worth noting here that this type of coordination has been found for *Complex-II* in the solid state by X-ray diffraction, as will be discussed later.

An important issue is to decide if the OH groups of the sugar units are deprotonated in the complexes. To answer this question,

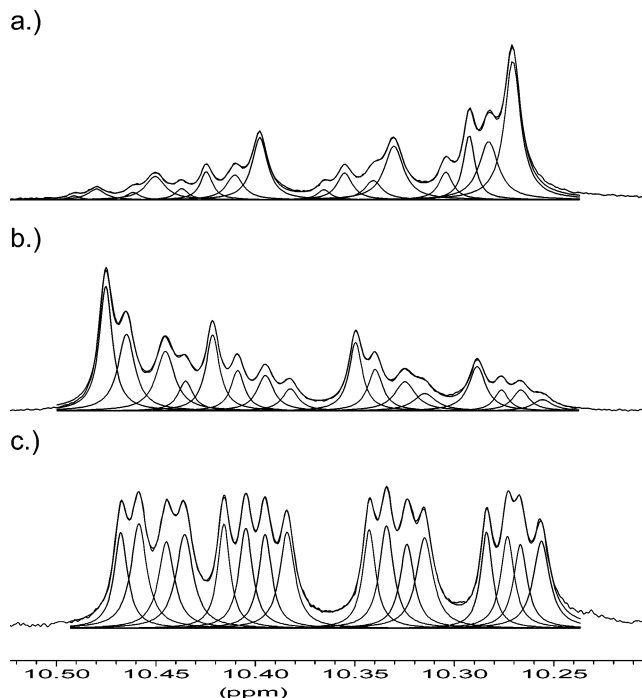


**Figure 5.** Deconvolution for the proton-decoupled  $^{31}\text{P}$  NMR signals observed for "Site- $\alpha$ " in *Complex-I*. The spectra are measured in the ternary U(VI) (50 mM)-AMP-CMP systems with different AMP:CMP ratios at pH = 9.4. The AMP and CMP concentrations (in mM) are (a) 9.6 and 23.9, (b) 19.2 and 9.4, and (c) 15.1 and 15.2.

it is worth mentioning that the formation of oxo or hydroxo bridges is quite common for the uranyl complexes at neutral or alkaline pH.<sup>39</sup> Especially, hydrolysis reactions of the uranyl ion, which begin already at pH = 3, result in a number of polymeric

species with oxo or hydroxo bridges linking the uranyl ions. It has also been reported that alkoxide or aryloxy ligands can form polynuclear complexes with bridging oxo ligands.<sup>40,41</sup> In addition, we have recently studied the complex formation and structure of uranium(VI) with  $\alpha$ -hydroxycarboxylic acids by NMR spectroscopy and potentiometry.<sup>42</sup> There we have found that oxo-bridged complexes were formed by proton dissociation from the  $\alpha$ -hydroxy group already around pH 3, indicating a dramatic increase, at least a factor of  $10^{13}$ , of its dissociation constant on coordination to uranium(VI). The same increase of the dissociation constant of the sugar OH groups and subsequent deprotonation upon chelate formation with the uranyl ion take place in the systems investigated here, as supported by the consumption of NaOH during the sample preparation. As shown by the spectra in Figure 3, the deprotonation of the sugar OH is indeed complete at pH = 9.44. Hence, the corresponding  $pK_a$  values must be  $\leq 9$ . Using the known uranium-to-nucleotide ratios for the complexes, their equilibrium constant is given by eqs 1 and 2.



$$K = \frac{[\text{Complex-II}]^2 [\text{H}^+]^m}{[\text{Complex-I}] [\text{L}]^2} \quad (2)$$

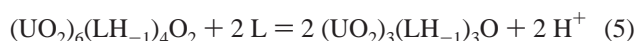
where [L] is the concentration of the free nucleotide and  $m$  is the number of released protons in the reaction. Equation 2 can be rearranged as

$$Y = m(-\log[\text{H}^+]) + \log K \quad (3)$$

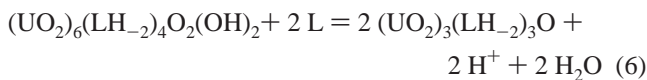
where

$$Y = 2(\log[\text{Complex-II}] - \log[\text{L}]) - \log[\text{Complex-I}] \quad (4)$$

Hence,  $m$  can be calculated from the slope of  $Y$  against the negative logarithm of the equilibrium hydrogen ion concentration. Linear regression to  $Y$ , calculated from the integrals of the <sup>31</sup>P NMR spectra recorded in the binary AMP system at five different pH values (Figure 3), yields the logarithmic value of the equilibrium constant,  $-16.6 \pm 0.8$  for eq 3, and the slope  $m = 1.9 \pm 0.2$  (Supporting Information, Figure S5), indicating the release of two protons in eq 1. Taking this into account, the equilibrium between the complexes can be written in two different ways depending on the number of released protons from the free ligand upon coordination. On the basis of the very similar chemical shifts of the coordinated nucleotides, we assume that these are bound in the same way at the same degree of deprotonation in both complexes. Hence, in the case when only one sugar OH is deprotonated, the equilibrium can be written as



while if both OH groups are deprotonated we have instead



with two hydroxide bridges in *Complex-I* (note that the charges are neglected for simplicity).

To make a proper choice for the stoichiometries of *Complex-I* described by eqs 5 and 6, one should consider the following. As discussed before, there must be two symmetric units in this complex consisting of three uranyl ions linked by a single oxide. According to the stoichiometry in eq 5, the two units can only be bonded by bidentate, bridging coordination of two of the phosphate groups, as shown in Figure S6, structure V. However, simple molecular modeling clearly shows that this type of coordination is not feasible geometrically for these ligands. Hence, it is more plausible to assume that the two units are connected via two hydroxide bridges and to assume a two-step deprotonation of nucleotides upon coordination according to eq 6, as presented in Scheme 3, structure I.

To decide if *Complex-I* contains coordinated water, we repeated some experiments using fluoride as a third ligand. As it has been demonstrated earlier, the fluoride ion forms stable complexes with uranium(VI) and can replace the coordinated water, but cannot replace bridging hydroxides in ternary systems, providing additional structural information.<sup>42,43</sup> However, in the <sup>19</sup>F NMR spectra of the uranium(VI)-AMP-F system, recorded using a large excess of fluoride, no coordinated fluoride signal could be observed, indicating no water coordination in *Complex-I*.

**2. <sup>17</sup>O NMR Spectra.** As mentioned before, the uranyl ion has two chemically inert oxygen ligands. The photochemically induced <sup>17</sup>O enrichment of these “yl”-oxygens<sup>32</sup> makes <sup>17</sup>O NMR spectroscopy particularly useful in studying the complex formation of uranium(VI) as demonstrated below. In the binary AMP (Figure 6) and CMP systems (Figure S7) two <sup>17</sup>O peaks with the same intensity can be observed for the uranyl oxygens in *Complex-II*. (One should keep in mind that all <sup>17</sup>O peaks in these spectra are arising from the oxygen in the  $\text{UO}_2^{2+}$  units, which, for simplicity, are assigned as “U” in Schemes 2 and 3.)

The fact that two signals with a relatively large difference in their chemical shifts appear indicates that the chemical surroundings for the two “yl”-oxygens are different. This can be explained by the steric interaction of one of the closely spaced phosphate oxygen atoms and one of the uranyl oxygens. As discussed later, crystallographic data for *Complex-II* show significant differences in the distances between the two “yl”-oxygens on the uranium atom and the two corresponding nonbonding oxygens of the phosphate group. For example, the distances between O(1A)–O(1P1) and O(1B)–O(2P1) are 3.96(5) and 4.97(5) Å, consequently. Similar “nonequivalence” of the uranyl <sup>17</sup>O signals has been recently observed in the uranium(VI)-*N*-phosphonomethyl-glycine system.<sup>43</sup>

In *Complex-I* two sets of two <sup>17</sup>O signals with a ratio of 2:1 can be observed, as indicated in Figures 6 and S7. The reason for the appearance of two sets of signals is the same as for *Complex-II*. However, the existence of two peaks within these sets indicates a difference in the coordination mode of the uranyl ions in *Complex-I*. It seems that the chemical shifts for two of

(39) Grenthe, I.; Fuger, J.; Konings, R. J. M.; Lemire, R. J.; Muller, A. B.; Nguyen-Trung, C.; Wanner, H. *Chemical Thermodynamics of Uranium*; North-Holland: Amsterdam, 1992; Vol. 1.

(40) Wilkerson, M. P.; Burns, C. J.; Dewey, H. J.; Martin, J. M.; Morris, D. E.; Paine, R. T.; Scott, B. L. *Inorg. Chem.* **2000**, *39*, 5277.

(41) Wilkerson, M. P.; Burns, C. J.; Morris, D. E.; Paine, R. T.; Scott, B. L. *Inorg. Chem.* **2002**, *41*, 3110.

(42) Szabó, Z.; Grenthe, I. *Inorg. Chem.* **2000**, *39*, 5036.

(43) Szabó, Z. *J. Chem. Soc., Dalton Trans.* **2002**, 4242.

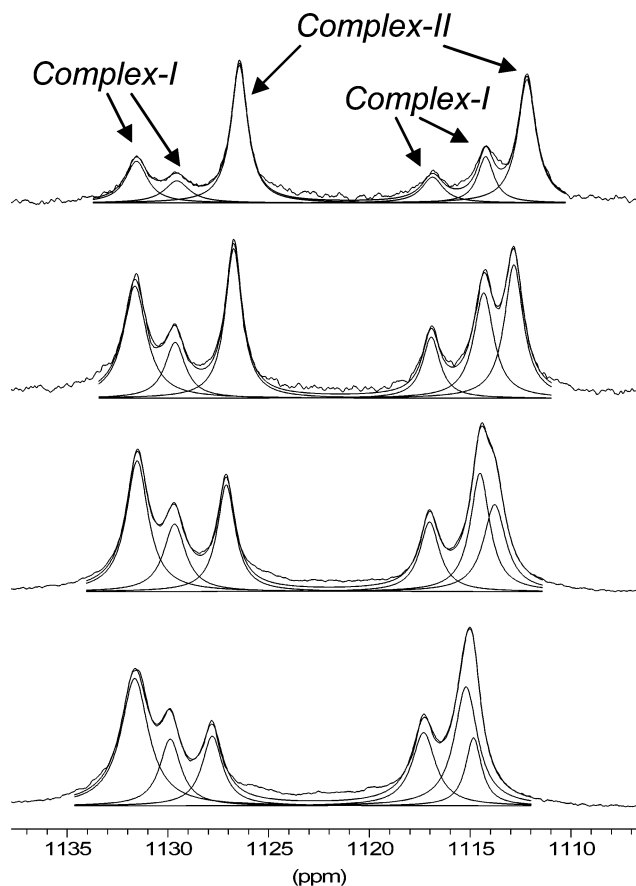


**Figure 6.** pH dependence of the  $^{17}\text{O}$  NMR spectra measured in the binary U(VI)-AMP system at 52 mM uranium(VI) and 53 mM AMP concentrations. The pH from top to bottom: 10.58, 10.15, 9.68, and 9.44.

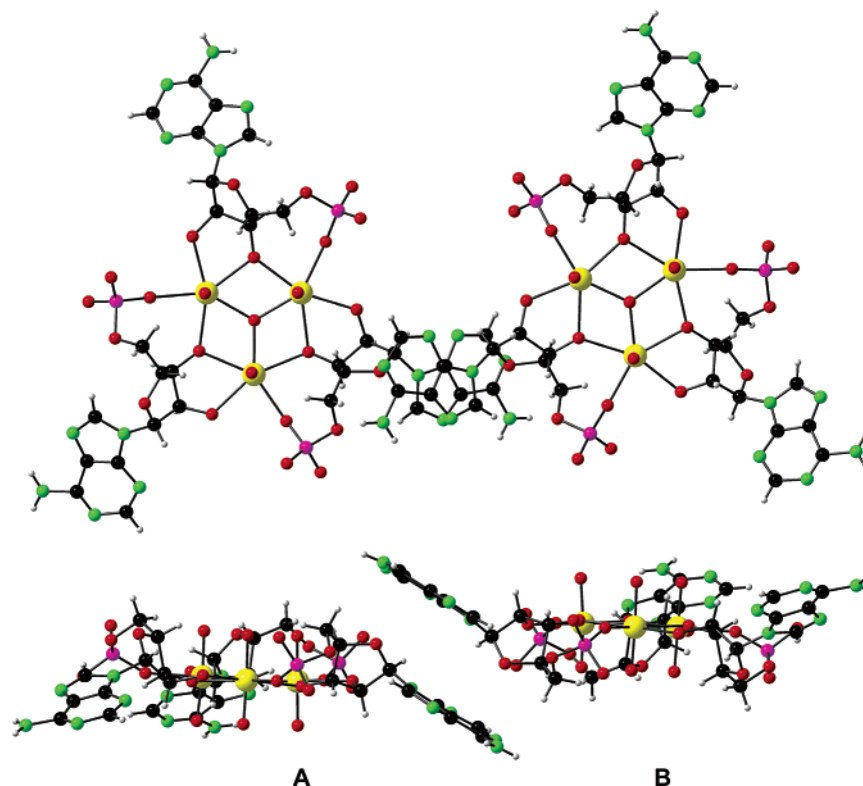


**Figure 7.** Two symmetry-independent trimeric molecules in the crystal structure of *Complex-II*. The adenine moieties are forced to adopt different orientations in the neighboring A and B entities. Views are parallel (top) and perpendicular (bottom) to the linear  $\text{O}=\text{U}=\text{O}$  axis. (Atomic labels are shown in Figure 8.)

the oxygens in the uranyl ions are determined by the coordination of both the phosphate group and the hydroxo- or oxo-bridges, while in the third one only by the hydroxo- or oxo-bridges.

**3.  $^{31}\text{P}$  NMR Spectra.** As mentioned before, characteristic  $^{31}\text{P}$  chemical shift differences can be observed for the two coordination sites in *Complex-I*. It can be seen that the chemical shift of the phosphorus atom in “*Site- $\alpha$* ” is strongly affected by the nature of the neighboring ligand in “*Site- $\beta$* ”. The  $^{31}\text{P}$  chemical shift of the ligand in “*Site- $\alpha$* ” is higher when AMP is coordinated in “*Site- $\beta$* ” than CMP (see Figures 4c and S3). This is most likely due to the difference in the shielding caused by the anisotropy of the aromatic N-heterocycles close to the phosphate group. This is expected to be larger for the bicyclic purine ring in AMP than that for the pyrimidine ring in CMP.

For the ligands in “*Site- $\beta$* ” only eight  $^{31}\text{P}$  signals can be observed in the resolution-enhanced spectra (Figure 4c), which indicates that the chemical shift of the phosphates here is less affected by the ligands coordinated in “*Site- $\alpha$* ”. Molecular modeling shows that the four uranium atoms bound by the hydroxide bridges are not in one plane, even if the complex, for simplicity, is drawn like that in Scheme 3. It also shows that the plane determined by two of the uranium atoms and the triple-bridged oxygen atom (bound to them and the third uranium atom) is not in the same plane as that determined by the corresponding atoms in the “other half” of the complex. Consequently, this geometry results in a larger distance between the phosphate groups in “*Site- $\beta$* ” and the heteroaromatic ring in “*Site- $\alpha$* ”, than that between the phosphate groups in “*Site- $\alpha$* ” and the heterocycle in “*Site- $\beta$* ”. This explains why the chemical shifts of these phosphates (“*Site- $\beta$* ”) are less affected by the anisotropy of the nucleobase in “*Site- $\alpha$* ”.

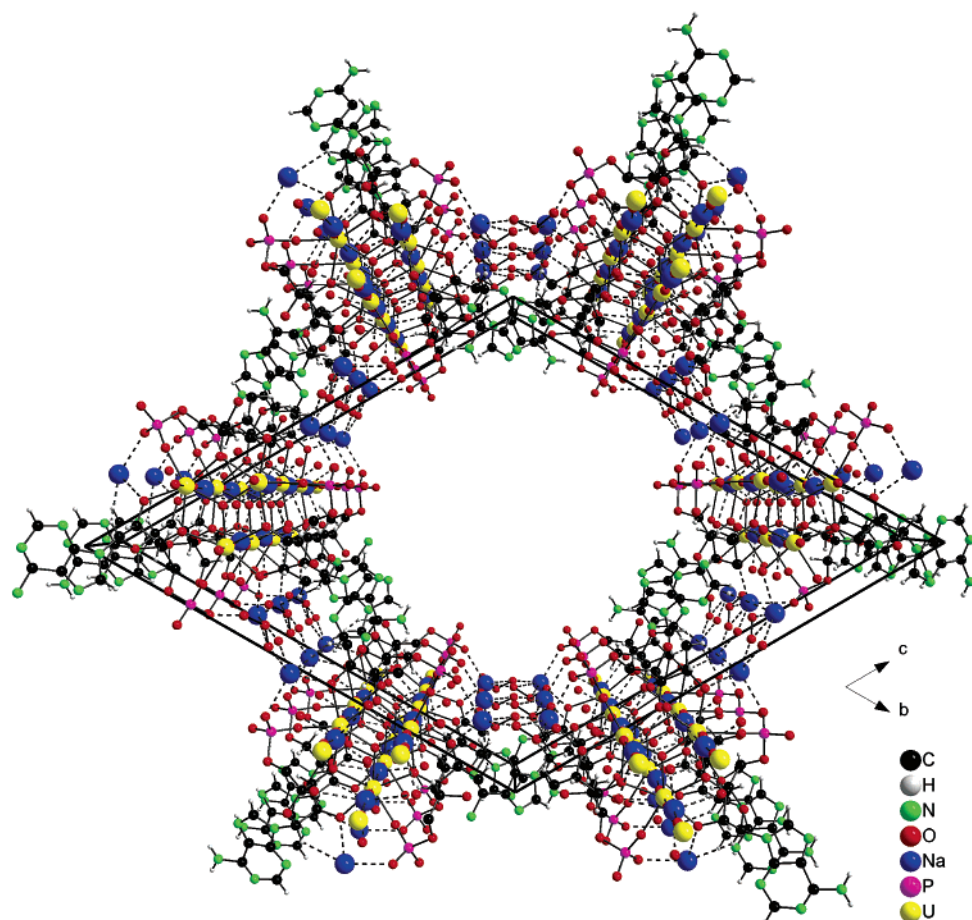


**Figure 8.** View of the crystal structure of *Complex-II* along the crystallographic *a* axis showing the formation of a hexagonal channel.

**4. Crystallographic Description of *Complex-II*.** The X-ray structure analysis proved the existence of the trimeric core for *Complex-II* (Figure 7), as suggested by the NMR results in aqueous solution (Scheme 3).

The crystallographic unit cell contains two symmetry-independent trimeric *Complex-II* entities (A and B), completed with sodium counterions and water molecules. In the crystal the complex entities are connected and held together by an intricate network of  $\text{Na}^+$  ions and water molecules, the latter ones forming a great number of hydrogen bonds. Uranyl groups, related by the symmetry operation  $x \pm 1, y, z$ , are connected via the positive counterions. Accordingly, the six sodium ions Na(1)–Na(6) form linear O–Na–O bridges between oxygens of the uranyl groups of U(1)–U(6), respectively. In this way columns are produced in the crystal that run parallel with each other in the crystallographic *a* direction. The stacks of the trimeric entities, containing either complex A or B, are arranged in a way so as to form hexagonal channels parallel with the columns along the crystallographic short *a* axis, as presented in Figure 8.

To make it possible for the stacks to come close enough to each other, the protruding flat, semirigid adenine moieties are forced to adopt different orientations in the neighboring A and B columns, with respect to the core of the respective complex. As a consequence, the symmetry of the packing arrangement decreases, but, at the same time, the possibility of close connections between neighboring complex entities in the *bc* plane increases, which in turn leads to increased packing density

and hence higher crystal stability. Also one of the oxygens in each phosphate group [O(1P1)–O(1P6)] may be connected to a  $\text{Na}^+$  ion [Na(7)–Na(12)], whereas the  $-\text{NH}_2$  groups of the six adenine moieties seem to form N–H $\cdots$ O bonds with included crystal water molecules. The sodium ions are then coordinated by water oxygens, which in turn may be involved in connection to other sodium ions and/or in hydrogen bonds to surrounding water molecules. It is worth mentioning that the network between the complex entities proved to be heavily disordered at room temperature. The Na(7)–Na(12) positions are only partially occupied (sof's ranging from 40 to 44%), and the adenine amine groups as well as the crystal water molecules exhibit high mobility and/or disorder in the studied crystal.

## Conclusion

Two sets of central conclusions can be drawn from our results: one in the structural and one in the methodological direction. On the structural side, after clarifying entangled and previously misinterpreted issues of the complex formation in the uranium(VI)-nucleotide systems, we are finally in the position to answer a question of large practical importance: the lack of catalytic activity of the uranyl ion in the internucleotide bond formation. According to our results, two stable, polynuclear complexes are formed in the alkaline pH range by the coordination of the 5'-phosphate group and the 2'- and 3'-hydroxyl groups of the sugar unit. The structures and the thermodynamic stabilities of the corresponding complexes are independent of the nucleotide type. At lower pH, the phosphate group and the

3'-hydroxyl group are the primary coordination sites in nucleotides. In this structure, a catalytic process resulting in 2'-5'-internucleotide formation is possible because the uranyl ion acts as a template, where the noncoordinated 2'-OH group can be activated by an internal hydrogen bond to the 3'-oxo group, as suggested by Sawai et al.<sup>12</sup> However, the formation of the complexes at higher pH, which are different from those proposed earlier, will prevent a uranyl-ion-catalyzed formation of oligonucleotides. The structural findings may also have some bearing on the assumedly complex scenario that is behind the dramatic decrease of the uranyl-catalyzed photocleavage of nucleic acids above pH = 8.5.

The NMR method that we invented to elucidate the structure may find many other applications in the chemistry of associating or self-associating systems. Although straightforward, to our knowledge there have been no previous application and independent validation of this combinatorial approach. Here, we achieved a full convergence of NMR and X-ray-crystallography derived structural information.

**Acknowledgment.** This study has been supported by the Swedish Research Council (VR) and the Carl Trygger Foundation. The authors thank Professor Ingmar Grenthe for helpful comments and valuable discussions.

**Supporting Information Available:** The crystallographic numbering of the core atoms in *Complex-II* (Figure S1a,b), various 2D homo- and heteronuclear correlation spectra (Figure S2a–f), structure of the isomers formed in a mixture of two nucleotides for *Complex-I* and the graphical representation of their <sup>31</sup>P chemical shift order in “Site- $\alpha$ ” (Figure S3), two other symmetric, but less feasible structures for *Complex-II* (Figure S4), linear regression of the pH dependence according to eq 3 (Figure S5), a possible, but less feasible structure for *Complex-I* (Figure S6), pH dependence of the <sup>17</sup>O NMR spectra measured in the binary U(VI)-CMP system (Figure S7), and X-ray crystallographic file for *Complex-II* in CIF format. This material is available free of charge via the Internet at <http://pubs.acs.org>.

JA0550273